Cement & Concrete Composites 26 (2004) 853–859

Cement & Concrete Composites

www.elsevier.com/locate/cemconcomp

Damage effects on concrete performance and microstructure

Parviz Soroushian *, Mohamed Elzafraney

Civil and Environmental Engineering Department, Michigan State University, 3546 Engineering Building, East Lansing, MI 48824-1226, USA

Received 2 July 2002; accepted 5 June 2003

Abstract

Changes in concrete properties and microstructure associated with different damaging effects were investigated. The damaging effects considered were induced by the exposure of concrete specimens to compression, impact, fatigue, and freeze–thaw cycles in saturated conditions. The influence of these damaging effects on the flexural strength, impact resistance, permeability and the extent and nature of microcrack propagation in concrete were investigated. Normal-strength and high-strength concrete materials were considered; the trends in damaging effects on concrete properties were justified based on microscopic observation of the trends in microcrack growth under such damaging effects.

Keywords: Concrete; Damage; Microstructure; Microcracks; Engineering properties

1. Introduction

Microcracks exist at cement paste–aggregate interfaces within concrete even prior to any load and environmental effects. Such microcracks are formed due to drying and thermal shrinkage mismatch of aggregate particles and cement-based matrix. Under externally imposed structural loads and environmental effects, concentration of tensile stresses occurs at the interfaces between aggregates and matrix, causing the growth of microcracks in size and number; propagation of interface microcracks into matrix and eventual joining of microcracks yield large cracks and lead to failure of concrete.

The growth of concrete microcracks under damaging load and environmental effects causes deterioration of concrete properties. Gettu et al. [1] reported that concrete tensile strength decreased significantly due to compression loads applied along a perpendicular direction. The drop in dynamic modulus of elasticity of concrete under freeze–thaw cycles is well known [2]. Permeability of concrete is also found to increase under repeated freeze–thaw cycles [2,3]. Zhang [4] detected an increase in pore specific surface area under flexural fatigue.

Many techniques have been employed to study the complex and heterogeneous microstructure of concrete [5]. These techniques include interferometry [6], acoustic emission [7], neutron radiography [8], mercury intrusion porosimetry [9], and optical and scanning electron microscopy [10–12]. Due to remarkable developments in microscopy and image analysis in recent decades, strong tools are now available for thorough assessment of concrete microstructure by microscopic means [13]. The study reported herein uses microscopic observation of microcrack propagation in concrete to explain the effects of various damaging phenomena on the engineering properties of concrete.

2. Experimental methodology

2.1. Concrete mixtures and test specimens

Two concrete mixtures were considered in the experimental program: (1) normal-strength; and (2) “relatively” high-strength. Type I Portland cement and natural sand were used in all mixtures. Crushed limestone with maximum particle size of 19 mm (3/4 in.) was used as coarse aggregate in the normal-strength mix. The high-strength mix incorporated natural granite with maximum particle size of 10 mm (3/8 in) as coarse aggregate; it also incorporated silica fume and small amount (1% by weight of cement) of water-reducing

* Corresponding author. Tel./fax: +1-517-355-2216.
E-mail address: soroushi@egr.msu.edu (P. Soroushian).

0958-9465/$ - see front matter © 2003 Elsevier Ltd. All rights reserved.
doi:10.1016/j.cemconcomp.2003.05.001

Table 1
Mix proportions (by weight) of normal-strength and high-strength concrete mixtures

Mixture	Ingredients					Air content	Targeted compressive strength MPa (psi)
	Type I Portland cement	Fine aggregate	Coarse aggregate	Water	Silica fume		
Normal-strength	1.00	1.59	1.98	0.514	0.00	3.5%	33 (4780)
Relatively high-strength	1.00	1.70	0.9	0.420	0.20	1.5%	45 (6520)

Table 2
Concrete specimens prepared from different mixtures

Specimen geometry and dimensions	Tests
102 mm (4 in.) diameter × 203 mm (8 in.) length cylinders	Compression
76 × 76 × 305 mm (3 × 3 × 12 in.) prisms	Flexure, compression, fatigue, freeze–thaw
152 mm (6 in.) diameter × 63.5 mm (2.5 in.) length cylinders	Impact
102 mm (4 in.) diameter × 51 mm (2 in.) length cylinders	Permeability

admixture "WRDA® 20". The mix proportions, targeted compressive strength and measured fresh mix air content of these two concrete mixtures are presented in Table 1. Table 2 presents the specimen prepared from these concrete mixtures. Molded specimens were kept moist for 24 h, after which they were demolded and moist cured at 100% relative humidity and 22 °C (72 F) for 28 days, and then conditioned (stored) at 50% relative humidity and 22 °C (72 F) for 180 days. Normal-strength and high-strength concrete specimens were kept moist for 24 h, after which they were demolded and then conditioned at 50% relative humidity and 22 °C (72 F) for 180 days. The main purpose of conditioning was to allow for drying shrinkage to cause microcracks which would occur over time in concrete systems.

2.2. Testing scheme

In order to assess how damaging phenomena affect concrete properties, two categories of tests were performed on concrete specimens: (1) control tests prior to any damaging effects; and (2) post damage tests after concrete specimens were exposed to various damaging phenomena. The control and post damage conducted in this investigation included compression (ASTM C39), flexure on prisms with a span of 228 mm (9 in.) under 4-point loading (ASTM C78), flexural fatigue between 15% and 85% of ultimate flexural strength at 450 cycles per minute (ACI Com. 215), drop weight impact (ACI Com. 544), and permeability (ASTM C1202).

The following tests were preformed on the two mixes:

1. compression, flexure, impact, fatigue, and permeability on normal-strength concrete; and
2. compression, flexure, impact, and permeability tests on high-strength concrete.

The following damaging phenomena were considered:

(1) Compression loading to peak stress with immediate unloading; (2) impact to 85% of the number of blows causing failure; (3) fatigue loading to 85% of the number of cycles causing failure; (4) 300 cycles (75 days) of freeze–thaw in water (ASTM C666); and (5) compression loading to peak compressive stress followed by immediate unloading and then exposure to 300 freeze–thaw cycles in water. These damaging phenomena left the specimens intact for the purpose of post-damage evaluation.

The test programs are summarized in Tables 3 and 4 for normal-strength and high-strength concrete, respectively. In order to assess the microstructural manifestations of damaging effects, two sections were cut parallel and perpendicular to loading direction for compression and flexure test specimens (or parallel and perpendicular to the longer dimension for freeze-thaw test specimens) as shown in Fig. 1. These sections were investigated through environmental scanning electron microscopy (ESEM) by means of backscattered technique. The contrast between microcracks/voids and the body of concrete was enhanced through Wood's metal impregnation. The following configuration was set up for ESEM: as accelerating beam voltage of 20 KV, an acquisition time of 30 s, and a vacuum of approximately 1×10^{-5} kg/cm^2 (1×10^{-6} Pa).

3. Experimental results

The effects of various damaging phenomena on flexural strength of normal-strength concrete are presented in Fig. 2. Reductions in flexural strength under different damaging effects range from 15% to 25%. Statistical

Table 3
The post-damage test program for the normal-strength concrete mix

Damaging effect	Post-damage tests	Specimens	Number of specimens
Compression	Flexure	Prism (76×76×305 mm)	4
	Impact	Cylinder (152×63.5 mm)	5
	Permeability	Cylinder (102×51 mm)	5
Impact	Permeability	Cylinder (102×51 mm)	5
Freeze–thaw	Flexure	Prism (76×76×305 mm)	3
	Permeability	Cylinder (102×51 mm)	3
Compression & Freeze–thaw	Flexure	Prism (76×76×305 mm)	2
Fatigue	Flexure	Prism (76×76×305 mm)	6

Table 4
The post-damage test program for the high-strength concrete mix

Damage conditions	Post-damage tests	Specimens types	Number of specimens
Compression	Flexure	Prism (76×76×305 mm)	3
	Impact	Cylinder (152×63.5 mm)	3
	Permeability	Cylinder (102×51 mm)	5
Impact	Permeability	Cylinder (102×51 mm)	5

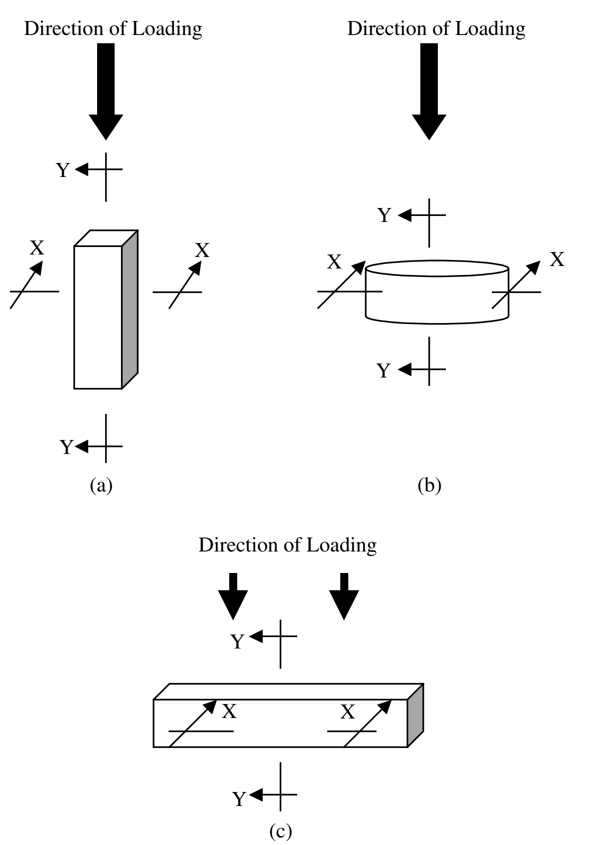

Fig. 1. Sectioning directions for microscopic investigations: (a) compression test; (b) impact and permeability tests and (c) flexure, fatigue, freeze–thaw, and different environmental exposure.

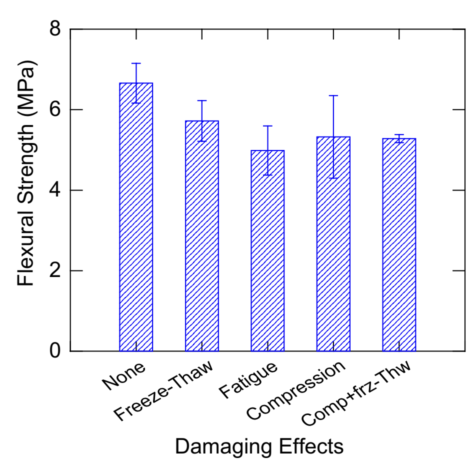

Fig. 2. Damaging effects on flexural strength of normal-strength concrete (means and standard errors).

analysis (ANOVA followed by pairwise comparison) of results indicated that there were statistically significant effects of compression (at 10% level of significance), compression + freeze-thaw (at 10% level of significance), fatigue (at 10% level of significance) and freeze–thaw (at 10% level of significance) on flexural strength. There was no statistically significant difference between different damaging effects on flexural strength of normal-strength concrete. In the case of high-strength concrete (Fig. 3), analysis of variance of test results indicated that the damaging effect of compression on flexural strength was

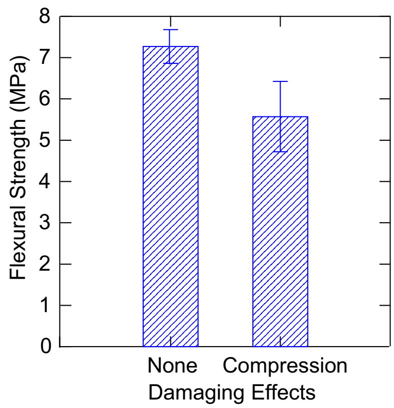

Fig. 3. Damaging effects of compression on flexural strength of high-strength concrete (means and standard errors).

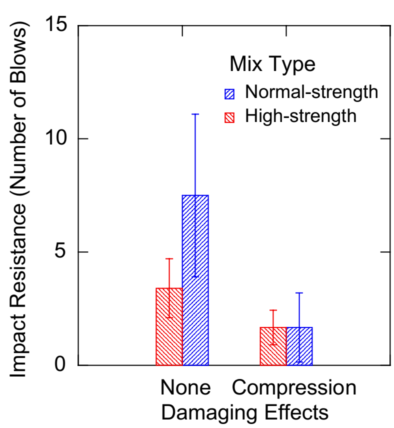

Fig. 4. Damaging effects of compression on impact resistance of normal-strength concrete (means and standard errors).

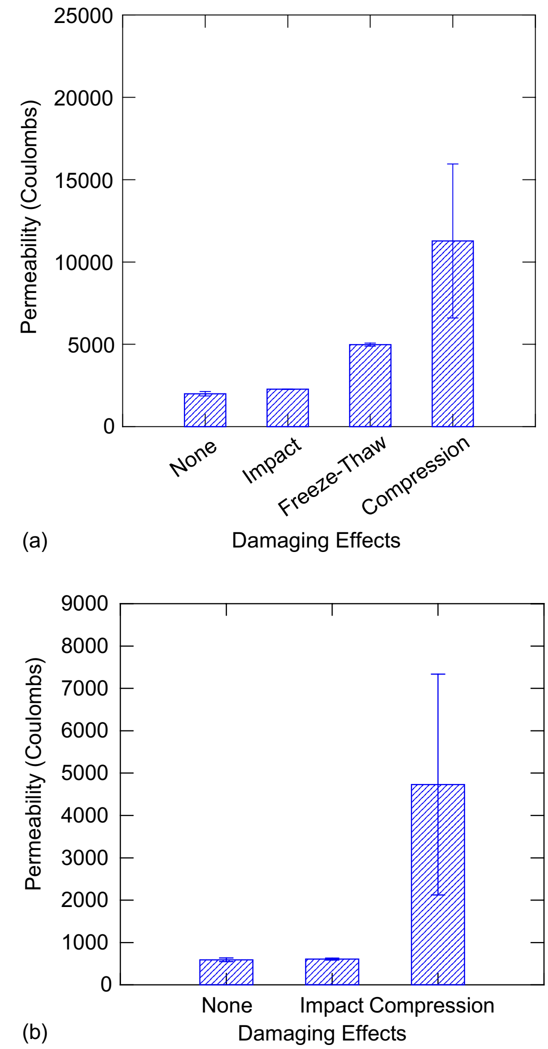

Fig. 5. Damaging effects on chloride permeability (means and standard errors): (a) normal-strength concrete and (b) high-strength concrete.

statistically significant at 5% level of significance. There was no statistically significant difference between the damaging effects of compression on flexural strength of normal-strength versus high-strength concrete (which suffered 20% and 21% loss of mean flexural strength, respectively, after compression loading). This may be attributed to the relatively small difference between the design strengths of the two concrete mixtures used in the current investigation. Fig. 4 presents the damaging effects of compression on impact resistance of normal-strength and high-strength concrete. Analysis of variance of the test data indicated that the damaging effects of compression on impact resistance of normal-strength and high-strength concrete were statistically significant at 5% level of significance. Normal-strength concrete seemed to suffer a greater loss of impact resistance than high-strength concrete after compression loading. As shown in Fig. 5, except for impact, other damaging effects seem to significantly increase the chloride permeability of both normal-strength and high-strength concrete. The variability of chloride permeability test results was, however, such that statistical analysis (ANOVA followed by pairwise comparison) of results indicated that only compression had statistically significant effects (at 5% level of significance) on chloride permeability of normal-strength and high-strength concrete.

4. Microstructural investigation

In order to investigate the microstructural manifestation of damaging effects, 24 four images were captured from each cross section; typical images, all captured at 125× magnification, are presented in Figs. 6 and 7 for normal-strength and high-strength concrete, respectively. The following observations were made on microscopic images. Damaging effects caused propagation and joining of microcracks within mixtures. Interfacial

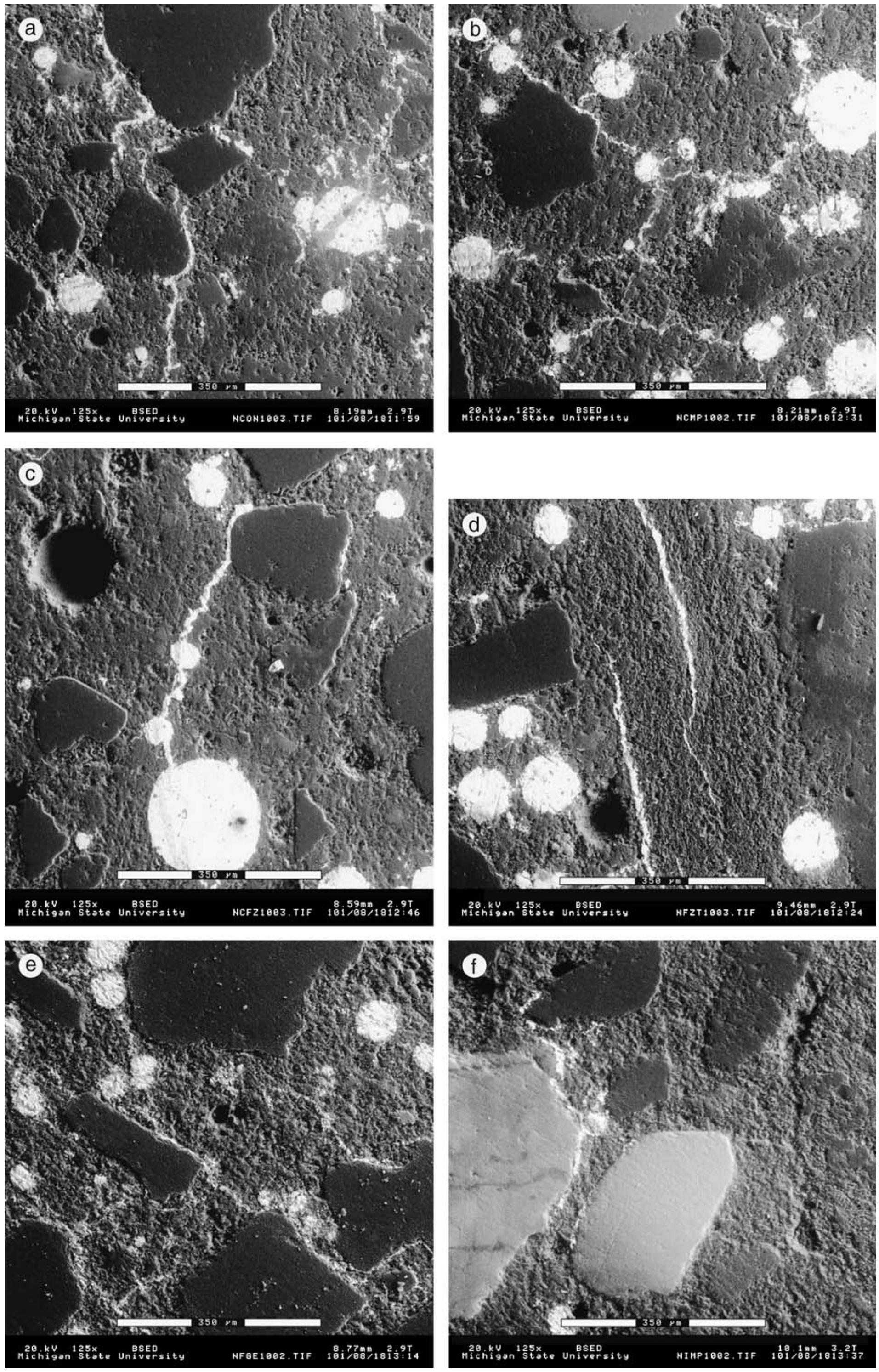

Fig. 6. Scanning electron micrographs for normal-strength concrete: (a) no damaging effect; (b) compression damaging effect; (c) compression + freeze–thaw damaging effect; (d) freeze–thaw damaging effect; (e) fatigue damaging effect and (f) impact damaging effect.

microcracks (at aggregate–paste interfaces) as well as some aggregate microcracks were present in concrete prior to any damaging effects as shown in Figs. 6a and 7a. Normal-strength concrete exhibited more extensive microcracking than high-strength concrete in undamaged condition. Drying and thermal shrinkage mismatch of cement paste versus aggregate explains interfacial microcracks. Compression loading caused propagation and networking of microcracks along interfaces and into the paste; the microcrack propagation path was rather

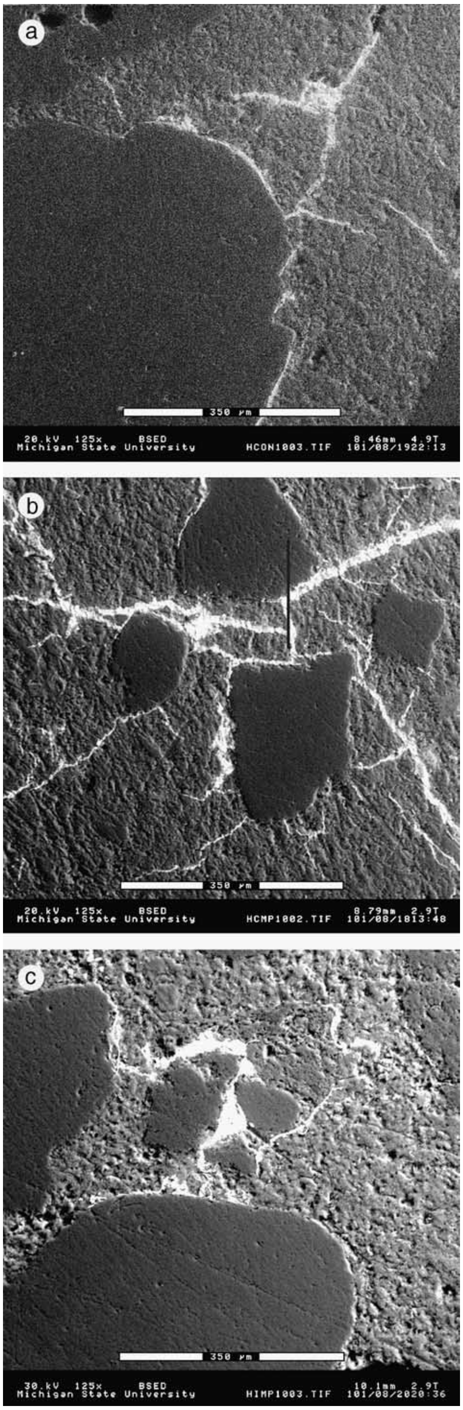

Fig. 7. Scanning electron micrographs for high-strength concrete: (a) no damaging effect; (b) compression damaging effect and (c) impact damaging effect.

tortuous as shown in Figs. 6b and 7b. Freeze–thaw effects on concrete specimens which were already subjected to compression did not substantially change the nature and extent of microcracking (see Fig. 6c). Freeze–thaw effect on undamaged specimens yielded less tortuous microcrack growth paths when compared with other damaging effects (see Fig. 6d). Fatigue loading seems to introduce more new microcracks as shown in Fig. 6e, when compared with other damaging effects which largely cause propagation of existing microcracks. It means that the energy required to create more new microcracks due to fatigue loading is less than the energy required to propagate existing microcracks. In concrete specimens subjected to impact, microcracks seem to be still limited to interfacial transition zones but their local widths seem to have grown when compared with undamaged specimens (see Figs. 6f and 7c). The extent of microcracking and the tortuosity of microcracks were less pronounced in high-strength concrete when compared with normal-strength concrete both prior to and after different damaging effects. Arresting and shifting of microcracks by voids and aggregates are occasionally observed in both normal-strength and high-strength concrete. In general it is noticed that there is no noticeable difference in microcrack density in parallel and perpendicular sections of undamaged specimens; after different damaging effects, however, differences appeared in microcrack intensity of the two perpendicular sections. In the case of compression and impact loading, sections perpendicular to the loading direction showed more intense microcracking than sections parallel to the loading direction.

5. Discussion

Various damaging effects produce different levels and types of microcrack propagation in concrete. There seem to be differences in tortuosity and number of microcracks (as well as the extent of microcracking) after different damaging effects. Post-damage properties of concrete reflect on these microstructural changes. For instance, the less tortuous nature of microcracks under freeze–thaw effect yields a relatively more significant effect on permeability than flexural strength. Quasi-static compression of concrete (to peak load) followed by immediate unloading produced extensive growth and interconnection of microcracks, thereby lowering the post-damage mechanical properties and transport properties of concrete. High-strength concrete exhibited less extensive interfacial microcracking in undamaged condition (before applying any damaging effect) when compared with normal-strength concrete; this could be attributed to differences in aggregate texture, water/cement ratio and interfacial bond strength between the types of concrete. Increased microcracking associated with damaging effects (e.g., compression) generally reduced the difference between properties of normal-strength and high-strength concrete. Microstructural investigations indicated that compression produces more intense microcrack growth than impact loading. Permeability measurements suggested that compression is far more damaging to transport properties of concrete than impact; this points at the correlation between the intensity of microcracking of the changes in key engineering properties after damaging effects. Microcrack analysis could thus be a valuable tool in condition assessment of deteriorated concrete structures.

6. Conclusions

Changes in concrete properties associated with various damaging effects were quantified. Observations were also made on microcrack attributes of concrete prior to and after such damaging effects. The results indicated that:

1. Different damaging effects (compression, impact, freeze-thaw, fatigue, freeze–thaw + compression) produced different changes in the extent and nature of microcrack propagation within concrete. Compression increased the length, width and area fraction of microcracks; fatigue increased the number of microcracks, freeze–thaw produced a less path of tortuous microcrack growth, and impact produced a more pronounced increase in microcrack width. Microcrack density increased noticeably in sections perpendicular to the loading direction when compared to the sections parallel to the loading direction.
2. Consecutive damaging processes do not always have adverse effects on concrete strength; for example, freeze–thaw damage effect and compression + freeze–thaw damage effect almost has the same influence on concrete flexural strength.
3. Differences in the extent and pattern of microcrack propagation reflected on the deterioration of different properties (flexural strength, impact resistance and permeability) of concrete after damaging effects.
4. Damaging phenomena do not have similar effects on different properties of concrete. Compression damage sharply increases permeability of concrete while impact damage has only slight effects on permeability. Compression damage also noticeably lowers the impact resistance of concrete. Fatigue loading was more damaging to flexural strength. Compression loading to peak followed by immediate unloading proved to be particularly damaging to concrete when compared with the other damaging phenomena considered in this investigation.
5. Microcrack propagation under compression damage seems to reduce the differences in properties of high-strength versus normal-strength concrete.

Acknowledgements

The work reported herein was conducted jointly by DPD, Inc. and Michigan State University under the sponsorship of the US Air Force.

References

[1] Gettu R, Aguado A, Oliveira MOF. Damage in high-strength concrete due to monotonic and cyclic compression—a study based on splitting tensile strength. ACI Mater J 1996;93(6):519–23.

[2] Saito M, Ohta M, Ishimori H. Chloride permeability of concrete subjected to freeze–thaw damage. Cement Concr Comp 1994;16: 233–9.

[3] Konin A, Francois R, Arliguie G. Analysis of progressive damage to reinforced ordinary and high performance concrete in relation to loading. Mater Struct 1998;31:27–35.

[4] Zhang B. Relationship between pore structure and mechanical properties of ordinary concrete under bending fatigue. Cement Concr Res 1998;28(5):699–711.

[5] Young JF. The microstructure of hardened portland cement paste. In: Creep and shrinkage in concrete structures. New York: John Wiley & Sons; 1982. p. 3–22.

[6] Regnault P, Bruhwiler E. Holographic interferometry for the determination of fracture process zone in concrete. Eng Fract Mech 1990;3:29–38.

[7] Sakata Y, Ohtsu M. Crack evaluation in concrete members based on ultrasonic spectroscopy. ACI Mater J 1995;92(6):686–98.

[8] Samah HR, Hover KC. Influence of microcracking on the mass transport properties of concrete. ACI Mater J 1992;98(4): 416–24.

[9] Nilleson K, Broderesen K. Pores and cracks in cemented waste and concrete. Cement Concr Res 1992;22:405–17.

[10] Nilleson K, Broderesen K. Pores and cracks in cemented waste and concrete. Cement Concr Res 1992;22:405–17.

[11] Becker JM, Grousson S, Jourlin M. Surface state analysis by means of confocal microscopy. Cement Concr Comp 2001;23: 255–9.

[12] Livingston RA, Manghnani M, Prasad M. Characterization of portland cement concrete microstructure using the scanning acoustic microscope. Cement Concr Res 1999;29:278–91.

[13] St John DA, Polle AW, Sims I. Concrete petrography. New York: John Wiley & Sons; 1998. pp. 36–46.

Parviz Soroushian Fellow of ACI, is a Professor of Civil and Environmental Engineering at Michigan State University. His specialty is in materials engineering; he has authored more than 100 technical publications and holds 15 patents in this field. He is past Chair of ACI Committee 549.

Mohamed Elzafraney received his BS and MS degrees from Alexandria University, Egypt, and is currently a Ph.D. candidate in Civil Engineering Dept., Michigan State University. His research interests include concrete microstructure and concrete durability.